Journal of Alloys and Compounds 507 (2010) 21–25

Contents lists available at ScienceDirect

Journal of Alloys and Compounds

journal homepage: www.elsevier.com/locate/jallcom

Structural and optical properties of nanocrystalline Ni–Zn ferrite thin films

S.M. Chavan[a], M.K. Babrekar[c], S.S. More[b], K.M. Jadhav[c,*]

[a] Department of Physics, Netaji college of Science, Mohol, Solapur 413 213 (M.S.), India
[b] Department of Physics, Y.C.M., Tuljapur, Osmanabad 413 601 (M.S.), India
[c] Department of Physics, Dr. Babasasheb Ambedkar Marathwada University, Aurangabad, 431 004 (M.S.), India

ARTICLE INFO

Article history:
Received 24 February 2010
Received in revised form 21 July 2010
Accepted 27 July 2010
Available online 4 August 2010

PACS:
75.50.Gg, 81.15.−z, 78.67.Bf

Keywords:
Thin films
Chemical synthesis
X-ray diffraction

ABSTRACT

Nanocrystalline ferrite thin films of $Ni_{1-x}Zn_xFe_2O_4$ (with $x = 0.0–1.0$, in the steps of $x = 0.2$) were prepared successfully by chemical bath deposition (CBD) method using nickel (II) chloride, zinc (II) chloride and iron (II) chloride as a constituent materials. The prepared thin films were characterized by X-ray diffraction (XRD) technique, scanning electron microscopy (SEM), infrared spectroscopy (IR) and UV–vis spectrophotometer at room temperature. X-ray diffraction studies revealed the formation of single phase spinel structure of the film. The crystallite size was determined using Scherrer formula and it is found to be of the order of 16–20 nm. The surface morphological studies of the films under investigation were carried out by SEM technique. The SEM images were used to obtain grain size which is of the order of 32–36 nm. IR spectra show two prominent peaks around 600 cm^{-1} and 400 cm^{-1}. Optical studies were carried out using UV–vis spectrophotometer. The band gap values are varies from 1.55 eV to 1.66 eV for varying zinc composition. The experimental results show that, CBD method allows the synthesis of nanocrystalline $Ni_{1-x}Zn_xFe_2O_4$ films with cubic spinel phase.

1. Introduction

In recent years an impressive research work on the growth and characterization of ferrite thin film has been appeared in the literature due to their wide range of technological application in various field. The magnetic properties of ferrite thin films are very sensitive to growth process and the method used for the preparation. Ferrite thin films with the spinel structure are potentially interesting both, scientifically and academically. Ferrite thin films are very important for the fabrication of memory [1], sensors [2], microwave devices [3], etc., because of their important magnetic and electrical properties, high chemical stability [4] and easy preparation. Currently, various techniques for fabricating ferrite thin films are available, which include pulsed laser deposition [5,6], sputtering [7], ferrite plating [8], dip coating process [9], spray pyrolysis [10], electro deposition [11], etc. Compared to other methods chemical bath deposition method offer better compositional comfort, low temperature, short duration of processing, low cost, etc. This method is most economic, simple and convenient for the deposition of ferrite thin films.

Nickel ferrite is the most suitable material for device applications [12,13]. Nickel ferrite has a technological importance in electrical and magnetic industries and has been used as a highly reproducible humidity [14] and gas sensor material [15,16]. Nickel ferrite is known to have an inverse spinel structure. The substitution of Zn-ions in nickel ferrite can lead to an interesting magnetic structure. In bulk form, nickel–zinc ferrite has been studied for its structural, electrical and magnetic properties by many workers [17,18]. Nickel–zinc spinel ferrite is a very important magnetic material due to its high electrical resistivity, high saturation magnetization and high magnetic permeability. In the literature, studies on the nickel ferrite thin film synthesized via electrochemical method [11] and chemical bath deposition method [19] have been reported. Liu et al. [20] and Sun et al. [21] have fabricated Ni–Zn and Ni–Cu–Zn spinel ferrite thin films successfully by sol–gel method. Their results on Ni–Zn and Ni–Cu–Zn ferrite thin film shows excellent soft magnetic performance. However, to our knowledge zinc substituted nickel ferrite thin films synthesized by chemical bath deposition technique have not been studied in detail for its structural, magnetic and optical properties. Considering the importance of nickel and substituted nickel ferrite thin film for various applications, in the present work we have investigated the structural and optical properties of Zn substituted nickel ferrite thin films prepared by chemical bath deposition technique.

2. Experimental details

Alkaline bath for Ni–Zn ferrite thin films was prepared by AR grade chemicals using double distilled water. Bath consists of 0.1 M solution of $NiCl_2$, $ZnCl_2$ and 0.2 M solution of $FeCl_2$. These salts were used as a source of cations. Adding NH_4OH solution (source of oxygen ions) made the bath alkaline with pH as 10, as well as the complexing agent. The deposition was carried out on stainless steel sub-

* Corresponding author. Tel.: +91 02402403384; fax: +91 02402403113.
E-mail address: drkmjadhav@yahoo.com (K.M. Jadhav).

0925-8388/$ – see front matter © 2010 Elsevier B.V. All rights reserved.
doi:10.1016/j.jallcom.2010.07.171

strate of the size 50 mm × 15 mm × 0.25 mm as well as on glass substrate of the size 75 mm × 25 mm × 1.35 mm for optical studies. The metallic substrates were polished using zero fine grade polish paper to appear like mirror. It is then washed with detergent solution with the help of cotton and flowing water. It is etched with 2% dilute HCl for approximately 20 s and ultrasonically cleaned with double distilled water. Finally substrate was dried in air.

Samples with the chemical formula Ni_{1-x} $Zn_xFe_2O_4$ (x varying from 0.0 to 1.0 in steps of 0.2) were prepared by chemical bath deposition method. First, ultrasonically, cleaned stainless steel substrate was immersed in combined alkaline nickel (II) chloride, zinc (II) chloride, and iron (II) chloride solution bath. When the bath attains the temperature of about 60 °C, the precipitation of the mixed solution was started. During the precipitation heterogeneous reaction occurred on the substrate and deposition of $Ni_{1-x}Zn_xFe_2O_4$ took place on the substrate. The film formation started after about 15 min and completed within nearly 120 min at 60 °C. During the process nickel, zinc and iron hydroxides absorbed onto the substrate.

$$NiCl_2 + ZnCl_2 + 4NH_4OH \rightarrow Ni(OH)_2 + Zn(OH)_2 + 4NH_4Cl \quad (1)$$

$$FeCl_2 + 2NH_4OH \rightarrow Fe(OH)_2 + 2NH_4Cl \quad (2)$$

Afterwards, the substrate was rinsed with anionic precursor i.e. double distilled water at room temperature, where oxygen ions reacts with pre-absorbed nickel, zinc and iron hydroxide on the substrate to form Ni–Zn ferrite film and also to remove nickel, zinc or iron complex species. The films are dried in hot air flow which results into oxidation of some iron atoms from +2 oxidation state to +3 oxidation state to form iron oxyhydroxide as required to form Ni–Zn ferrite [22,23].

$$Fe(OH)_2 \xrightarrow[O_2]{\text{hot air drying}} FeOOH + H_2O \uparrow \quad (3)$$

The iron oxyhydroxide thus formed get mixed with the nickel hydroxide and zinc hydroxide to form the Ni–Zn ferrite thin film. The reaction mechanism is mentioned as below:

$$Ni(OH)_2 + Zn(OH)_2 + 2FeOOH \xrightarrow{450\ ^\circ C} Ni - Zn\ Fe_2O_4 + 3H_2O \uparrow + \frac{1}{2}O_2 \uparrow \quad (4)$$

The Ni–Zn ferrite thin films produced by CBD technique finally was annealed at 450 °C for 3 h to form pure Ni–Zn ferrite with cubic spinel phase, removing any hydroxide content and complete crystallization of the film takes place.

By changing deposition time on stainless steel substrate, the thickness of the film was controlled. Thickness of annealed Ni–Zn ferrite thin film was measured using thickness profiler AMBIOS (XP-1). The structural characterization of the prepared Ni–Zn ferrite film was carried out using X-ray diffraction technique in the 2θ range of 20–80° on Philips X-ray diffractometer, using Cu-Kα (λ = 1.5406 Å) radiations. The average crystallite size of the Ni–Zn ferrite thin film was estimated from the full width at half maximum (FWHM) of the most intense diffraction line (3 1 1) using Scherrer formula [24]. Microstructural study was accomplished using scanning electron microscopy (SEM). SEM images of the films were obtained on JEOL JSM-6360 unit. FT-IR spectrum was recorded using Perkin-Elmer infrared spectrometer model 783 in the range 350–1000 cm^{-1}. The optical absorption of the films was measured using a Systronic spectrophotometer −119.

3. Results and discussion

3.1. Film thickness

The properties of the ferrite thin films are sensitive to thickness of the film. The preparative parameters such as concentrations, deposition time period and temperatures. were optimized to obtain uniform thickness of the film. The film thickness obtained by using thickness profiler is typically between 0.4 μm and 3.5 μm depending upon the deposition time and temperature. The variation of film thickness as a function of deposition time for a typical composition $x = 0.6$ (when bath temperature is 60 °C) is shown in Fig. 1. It can be seen that the film thickness increases with deposition time up to 20 min and then remains constant for further increase in deposition time. The Ni–Zn ferrite thin film has maximum terminal thickness of about 3.5 μm. The optimized preparative parameters for Ni–Zn ferrite thin films are listed in Table 1. Using these optimized parameters, Ni–Zn ferrite thin films with varying composition has been prepared and was used for further characterization.

3.2. Structural analysis

X-ray diffraction studies were carried out on Ni–Zn thin films with a view to investigate structural properties. Fig. 2 represents XRD patterns for pure (a) $NiFe_2O_4$ ($x = 0.0$) and (b) $ZnFe_2O_4$

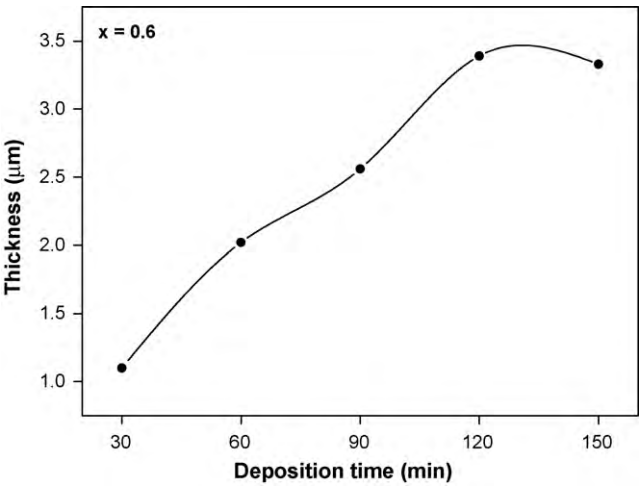

Fig. 1. Variation of thickness with deposition time for typical composition $x = 0.6$.

Table 1
Optimized preparative parameters for Ni–Zn ferrite thin films.

Concentration of cationic precursor	0.1 M $NiCl_2$ + 0.1 M $ZnCl_2$ + 0.2 M $FeCl_2$
Anionic precursor	H_2O
Complexing Agent	NH_4OH
pH of cationic precursor	~10
Deposition temperature	60 °C
Deposition time	120 min

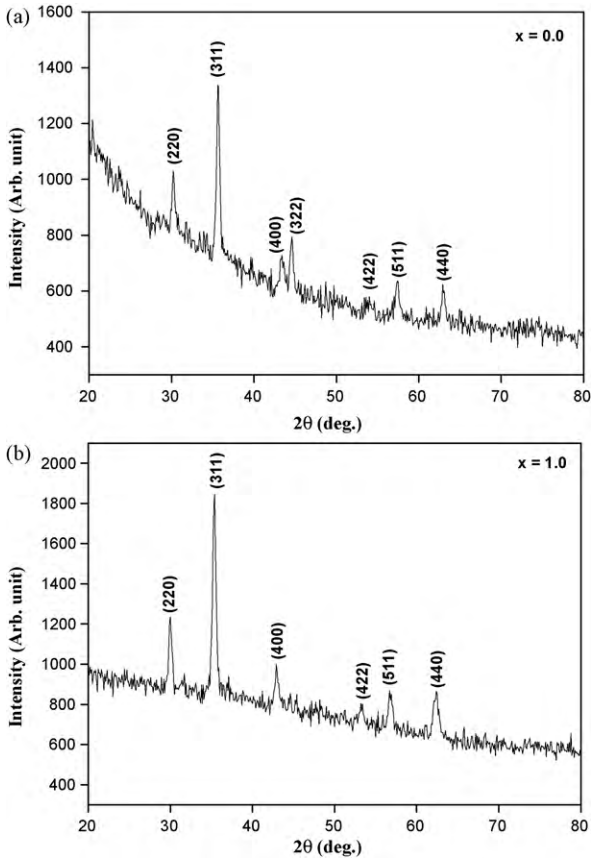

Fig. 2. XRD patterns for (a) $NiFe_2O_4$ ($x = 0.0$) and (b) $ZnFe_2O_4$ ($x = 1.0$).

Table 2
Values of lattice constant '*a*', crystallite size and grain size for Ni–Zn ferrite thin film.

Composition *x*	Lattice constant '*a*' (Å)	Crystallite size (nm)	Grain size (nm)
		XRD	SEM
0.4	8.339	18	–
0.2	8.351	20	–
0.4	8.356	18	–
0.6	8.397	20	32
0.8	8.403	18	36
1.0	8.426	16	–

($x = 1.0$). The XRD pattern shows the reflections corresponding to (2 2 0), (3 1 1), (4 0 0), (3 2 2), (4 2 2), (5 1 1) and (4 4 0), which are allowed peaks of the cubic spinel structure. The plane (3 1 1) is most intense whereas others are relatively low intense. The small peak intensities in XRD pattern, revealed the existence of fine grain nanocrystalline with most of the part as amorphous. The analysis of XRD pattern revealed the formation of single phase cubic spinel structure.

Using the XRD data, lattice constant '*a*' was determined and the values are presented in Table 2. It can be seen from the values of lattice constant that, lattice constant increases linearly with increase in zinc concentration *x*. The linear increase in lattice constant with Zn content obeys Vegard's law [25]. The increase in lattice constant is attributed to the fact that, the Ni^{2+} (0.74 Å) ions of smaller ionic radii are replaced by Zn^{2+} (0.84 Å) ions of larger ionic radii. Our results on the variation of lattice constant with Zn substitution are fairly agree well with those reported in the literature [17,26–28]. The variation of lattice constant with zinc substitution is shown in Fig. 3. The values of lattice constant for $x = 0.0$ and $x = 1.0$ i.e. for $NiFe_2O_4$ and $ZnFe_2O_4$ are in good agreement with the reported value of lattice constant [29].

The crystallite size of all the samples was obtained using the Scherrer formula given by:

$$t = \frac{0.9\lambda}{\beta \cos\theta} \quad (5)$$

where, λ is the X-ray wavelength, θ is the Bragg's angle and β is the full width of the diffraction line at half the maximum intensity.

The most intense peak (3 1 1) was considered for the determination of the full width at half maxima (FWHM). The values of crystallite size are given in Table 2. The crystallite size obtained from XRD data is of the order of 16–20 nm. Thus, the nanocrystalline formation of Ni–Zn ferrite thin film was confirmed from the values of crystallite size. The scanning electron microscopy studies were undertaken for the samples with $x = 0.6$(a) and $x = 0.8$(b), and

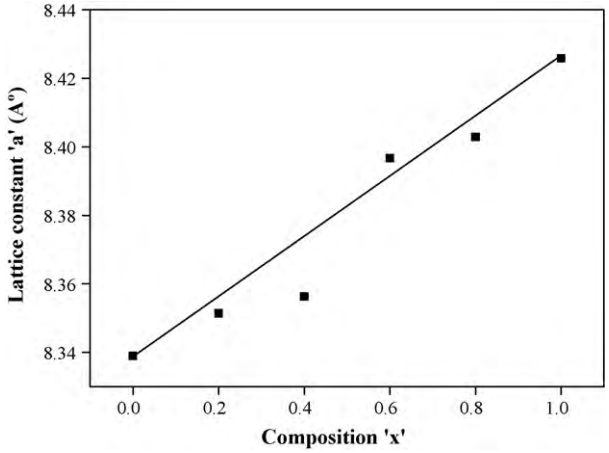

Fig. 3. Variation of lattice constant '*a*' with composition '*x*'.

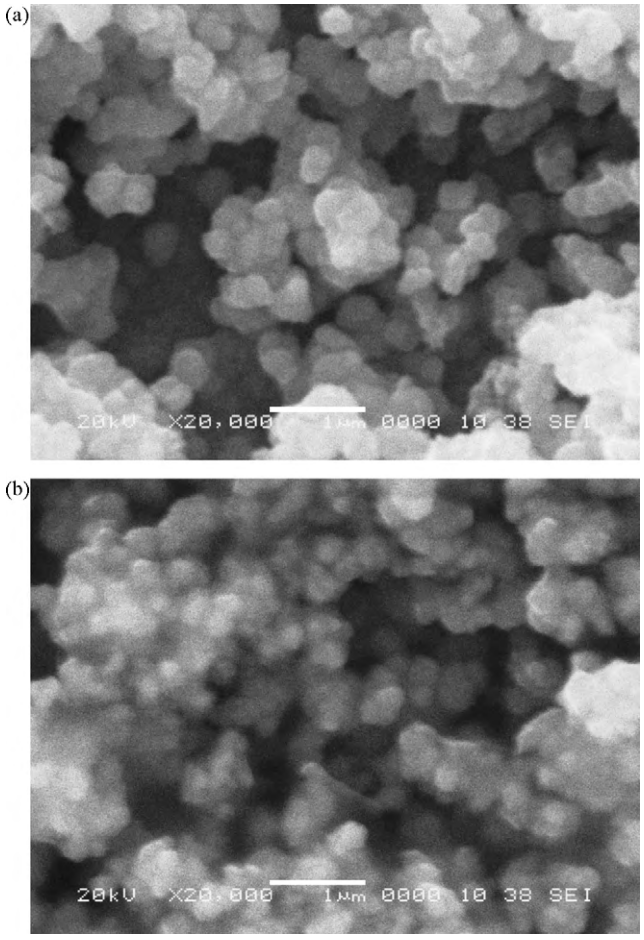

Fig. 4. SEM images for typical samples (a) $x = 0.6$ and (b) $x = 0.8$.

images are shown in Fig. 4. The SEM images clearly indicate the well grown grains. These SEM images are used to obtain the grain size. The grain size obtained from SEM images is also listed in Table 2.

3.3. FT-IR studies

The thin films of Ni–Zn spinel ferrites were characterized by infrared spectroscopy. Typical IR spectra for the samples with $x = 0.6$(a) and $x = 0.8$(b) are shown in Fig. 5. Two absorption bands are clearly seen in the IR spectra revealing the characteristic feature of spinel ferrite. IR spectra are similar to the other well known spinel ferrite [30]. The absorption bands are seen at around 400 cm^{-1} and 600 cm^{-1}, and are attributed to intrinsic vibrations due to tetrahedral (A) group and octahedral (B) group respectively. The values of absorption bands are given in Table 3. On the basis of FT-IR spectral results, it can be concluded that, chemical bath deposition (CBD) method results into deposition of single phase cubic spinel nanocrystalline Ni–Zn ferrites at relatively low temperature.

Table 3
Values of absorption bands (ν_1 and ν_2) for Ni–Zn ferrite thin films.

Composition *x*	Absorption bands	
	ν_1 (cm^{-1})	ν_2 (cm^{-1})
0.0	404.01	591.13
0.2	410.99	555.10
0.4	400.19	583.05
0.6	410.51	575.05
0.8	411.78	571.23
1.0	409.14	564.02

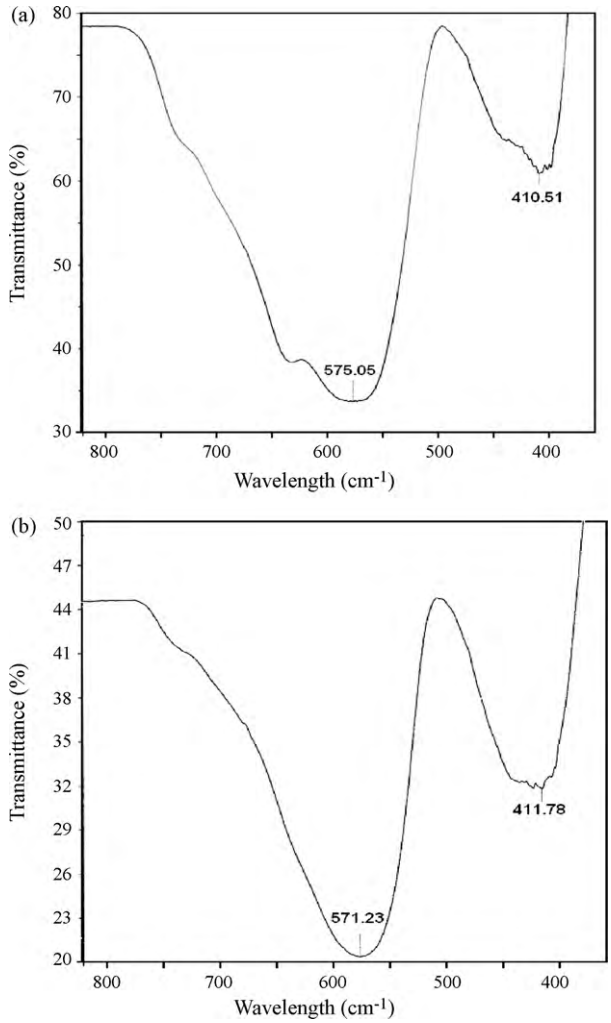

Fig. 5. IR absorption spectra of typical samples (a) $x = 0.6$ and (b) $x = 0.8$.

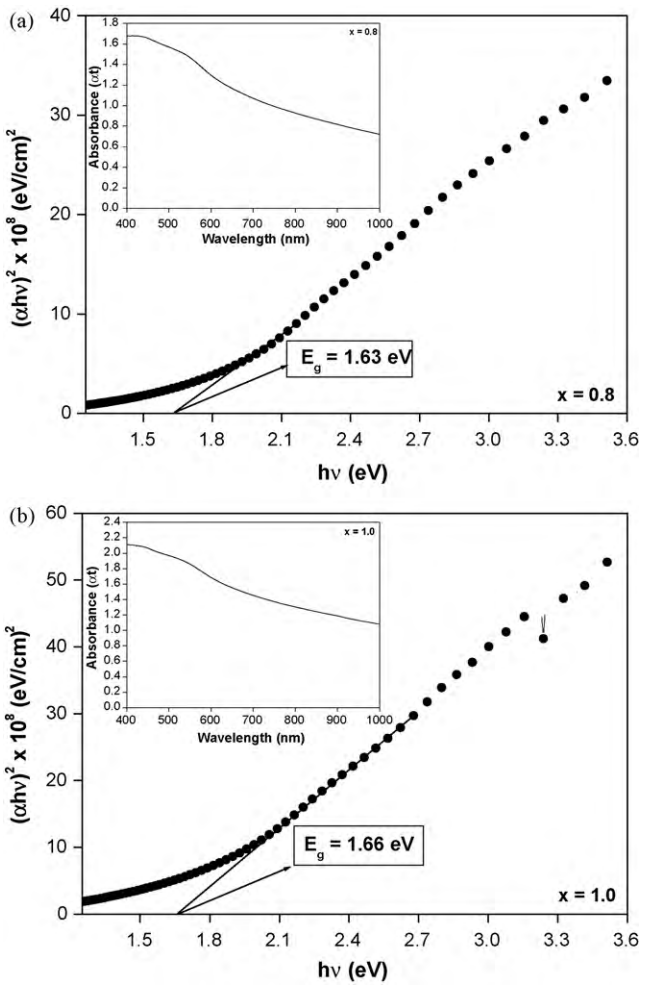

Fig. 6. Variation of absorbance with wavelength for typical samples (a) $x = 0.8$ and (b) $x = 1.0$.

3.4. Optical studies

The optical properties of Ni–Zn ferrite thin film deposited on glass substrate was studied using UV–vis spectrophotometer. The absorbance of the thin films deposited on glass substrate was measured in the wavelength range 400–1000 nm by substracting the absorbance of the glass substrate, which was taken as reference. The UV–vis characterization of the thin film was used to obtain band gap energy. The UV–vis absorbance spectra of Ni–Zn thin film on a glass substrate for typical samples ($x = 0.8$ and 1.0) is shown in inset of Fig. 6(a and b) respectively. The absorption is due to only ferrite nano-particles. The absorption spectrum reveals that the Ni–Zn ferrite thin films has low absorbance in visible region and close to infrared region, however, absorbance in UV region is high. Our result of the optical behavior is analogues to those reported by Bilecka et al. [31] for cobalt ferrite thin film synthesized via microwave assisted non-aqueous sol–gel process.

The UV–vis data were analyzed from the following classical relation for near edge optical absorption in semiconductors which gives relation between the optical band gap, absorption coefficient and energy ($h\upsilon$) of the incident photon.

$$\alpha = \frac{A(h\upsilon - E_g)^{n/2}}{h\upsilon} \quad (6)$$

where A is a constant independent of $h\upsilon$ [32], E_g is the semiconductor band gap and n is a number equal to 1 for direct gap and 4 for indirect gap compound. The plots of $(\alpha h\upsilon)^2$ versus $h\upsilon$ of the annealed films are shown in Fig. 6. Since the plots of $(\alpha h\upsilon)^2$ versus $h\upsilon$ are almost linear, the direct gap nature of the optical transition in Ni–Zn ferrite films is confirmed. The band gap energies were obtained by extrapolating the linear portion of $(\alpha h\upsilon)^2 - (h\upsilon)$ plot to the energy axis for zero absorption. The estimated band gap for compositions $x = 0.8$ and $x = 1.0$ are 1.63 eV and 1.66 eV. Fig. 7 shows

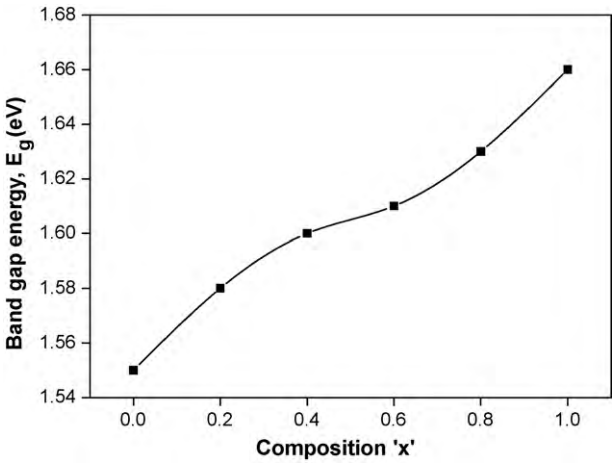

Fig. 7. Variation of optical band gap with different compositions 'x'.

the variation of optical band gap with different compositions x. It is observed from Fig. 7 that, the energy band gap increases with increase in Zn concentration. The band gap value is influenced by various factors such as film thickness, crystallite size, structural parameter, carrier concentrations, presence of impurities, and deviation from stoichiometry of the film and lattice strain [33]. The increase in band gap in the present case may be attributed to the increase in structural parameter (lattice constant) with Zn concentration. The band gap values (1.55–1.66 eV) were nearly equal to experimental values reported for bulk Ni–Zn ferrite material (1.50–1.66 eV) [34].

4. Conclusions

Successful deposition of nanocrystalline Ni–Zn thin film was carried out by chemical bath deposition (CBD) technique on a glass substrate. As deposited Ni–Zn films are amorphous. After annealing at 450 °C for 3 h Ni–Zn ferrite thin film with cubic spinel crystal structure was formed indicating the removal of hydroxide phase and completion of crystallization process as evidenced by XRD and FT-IR spectrum. It is observed from SEM images that the film covered the substrate well with a homogeneous and uniform surface. The band gap obtained from UV–vis data increases with Zn substitution suggesting that the structural change occurring in the composite is responsible for such a variation.

Acknowledgements

One of the authors, Mr. S.M. Chavan is very much thankful to Prof. C.D. Lokhande, Physics Department, Shivaji University, Kolhapur, M.S., India, for his kind help. Author is also thankful to Dr. J.L. Gunjkar, Physics Department, Shivaji University, Kolhapur, M.S., India, for his support to carry out research work.

References

[1] X. Sui, M.H. Kryder, Appl. Phys. Lett. 63 (1993) 1582.
[2] T. Kiyomura, Y. Maruo, M. Gomi, J. Appl. Phys. 88 (2000) 4768.
[3] B.Y. Wong, X. Sui, D.E. Laughlin, M.H. Kryder, J. Appl. Phys. 75 (1994) 5966.
[4] R. Valenzuela, Magnetic Ceramics, Cambridge University Press, Cambridge, 1994.
[5] M. Johnson, P. Kotula, C. Carter, J. Cryst. Growth 206 (1999) 299.
[6] B. Negulescu, L. Thomas, Y. Dumont, M. Tessier, N. Keller, M. Guyot, J. Magn. Magn. Mater. 242 (2002) 529.
[7] S. Venzke, R.B. Vandover, J.M. Phillips, E.M. Gyorgy, T. Siegrist, C.H. Chen, D. Werdr, R.M. Fleming, R.J. Felder, E. Coleman, R. Opila, J. Mater. Res. 11 (1996) 1187.
[8] M. Abe, Electrochim. Acta 45 (2000) 3337.
[9] T. Tsuchiya, H. Yamashirao, T. Sci, T. Inamura, J. Mater. Sci. 27 (1992) 3645.
[10] Y. Chung, S. Park, D. Kang, Mater. Chem. Phys. 86 (2004) 375.
[11] S.D. Sartale, C.D. Lokhande, M. Giersig, V. Ganesan, J. Phys. Condens. Matter 16 (2004) 773.
[12] K. Ishino, Y.A.M. Naramiya, Ceram. Soc. Bull. 66 (1987) 1469.
[13] Q. Zhang, T. Itoh, M. Abe, Y. Tamaura, in: T. Yamaguchi, M. Abe (Eds.), Ferrites Proc. ICF–6, Tokyo, 1992, p. 481.
[14] G.R. Dube, V.S.J. Darshane, Mol. Catal. 79 (1993) 285.
[15] C.V. Gopal Reddy, S.V. Manorama, V.J. Rao, Sens. Actuators B 55 (1999) 90.
[16] L. Satyanarayana, K. Madhusudan Reddy, S.V. Manoram, Mater. Chem. Phys. 82 (2003) 21.
[17] S.S. Jadhav, S.E. Shirsath, B.G. Toksha, S.J. Shukla, K.M. Jadhav, Chin. J. Chem. Phys. 21 (2008) 4.
[18] A.M. More, J.L. Gunjkar, C.D. Lokhande, R.S. Mane, S.-H. Han, Micron 38 (2007) 500.
[19] C. Prakash, J.S. Baijal, J. Less Commun. Met. 106 (1985) 257.
[20] F. Liu, C. Yang, T. Ren, A.Z. Wang, J. Yu, L. Liu, J. Magn. Magn. Mater. 309 (2007) 75.
[21] K. Sun, Z. Lan, Z. Yu, X. Nie, L. Li, X. Zhao, J. Mater. Sci. 44 (2009) 4348.
[22] A.A. Olowe, J.M.R. Genin, Corros. Sci. 32 (1991) 965.
[23] U.S. Patent no. 4.061.725. (Published date 12/06/1977).
[24] C. Venkataraju, G. Sathishkumar, K. Sivakumar, J. Magn. Magn. Mater. 322 (2010) 230.
[25] B.D. Cullity, Elements of X-ray Diffraction, vol. 99, Addison–Wesley Publ. Comp. Inc., Reading, MA, 1956.
[26] S.V. Kakatkar, S.S. Kakatkar, R.S. Patil, A.M. Sankpal, S.S. Suryawanshi, D.N. Bhosale, S.R. Sawant, Phys. Stat. Sol. (b) 198 (1996) 853.
[27] Y.G. Chukalin, V.R. Shirts, Phys. Stat. Sol. (a) 160 (1993) 185.
[28] D. Ravinder, G. Rangmohan, Mater. Lett. 44 (2000) 139.
[29] B. Vishwanathan, V.R.K. Murthy, Ferrite Materials Science & Tech., vol. 96, Narosa Publishing House, New Delhi, 1990.
[30] M. Gotic, I. Czako-Nagy, S. Popovic, S. Music, Philos. Magn. Lett. 78 (1998) 193.
[31] I. Bilecka, M. Kubli, E. Amstad, M. Niederberger, J. Sol–Gel Sci. Technol., doi:10 1007/s1097-010-2165-1. (published online).
[32] R.S. Rasu, G.I. Rasu, J. Optoelect., Adv. Mater. 7 (2005) 223.
[33] R.B. Kale, C.D. Lokhande, Appl. Surf. Sci. 223 (2004) 343.
[34] G.P. Joshi, N.S. Saxena, R. Mangal, A. Mishra, T.P. Sharma, Bull. Mater. Sci. 26 (2003) 387.